

PICARD LATTICES OF FAMILIES OF K3 SURFACES

SARAH-MARIE BELCASTRO
 DEPARTMENT OF MATHEMATICS
 UNIVERSITY OF NORTHERN IOWA
 CEDAR FALLS, IA, 50614-0506.
 EMAIL: SMBELCAS@MATH.UNI.EDU

ABSTRACT. Using toric geometry, lattice theory, and elliptic surface techniques, we compute the Picard Lattice of certain K3 surfaces. In particular, we examine the generic member of each of M. Reid’s list of 95 families of Gorenstein K3 surfaces which occur as hypersurfaces in weighted projective 3-spaces. As an application, we are able to determine whether the mirror family (in the sense of mirror symmetry for K3 surfaces) for each one is also on Reid’s list.

1. INTRODUCTION

Given an integral convex polytope Δ , we may associate to Δ a toric variety \mathbb{P}_Δ and a family of hypersurfaces X_Δ in \mathbb{P}_Δ , referred to as *toric hypersurfaces*. Generically, the members of the family are transversal to the parent variety and have only singularities inherited from \mathbb{P}_Δ (see [11]). The scope of this paper is limited to 2-dimensional toric hypersurfaces whose parent varieties are weighted projective spaces.

In 1979, M. Reid classified and listed all families of K3 weighted projective hypersurfaces with Gorenstein singularities (but did not publish this work). Yonemura [17] lists the weight-vectors for the associated weighted projective spaces for each of the 95 families of surfaces. This list of surfaces arises in many subfields of algebraic geometry, including singularity theory and the birational geometry of three-folds. The present work was originally motivated by a question of Dolgachev about K3 mirror symmetry on the “Famous 95” (see Section 6 for this application), but became focused on techniques for exhibiting and analyzing elliptic fibrations on K3 surfaces (see Sections 4 and 5 in particular).

1991 *Mathematics Subject Classification*. Primary 14J28, 14J27, 14C22; Secondary 14J32, 14Q10, 14D06, 14M25.

Key words and phrases. elliptic surface, K3 surface, Picard, toric, fibration.

We denote weighted projective space as $\mathbb{P}(q_1, q_2, \dots, q_n)$, where the q_i are the weights of the projective variables. In classifying the ‘‘Famous 95’’, the restrictions that the surfaces be K3 and Gorenstein determined which weight-vectors are possible. Thus, each of the 95 families may be defined by the weighted projective space in which it resides, as follows. Let S be a generic member of one of the 95 families.

The adjunction formula in weighted projective space (see [8]) induces the property that $\deg(S) = \sum_i q_i = s$. To construct the toric variety to which each family is associated, we will use the standard toric geometry correspondance between monomials $x^{\vec{p}_i}$ and integral lattice points \vec{p}_i . (Excellent references on toric varieties are [9] and [6].) We want the monomials of the family’s equation to have degree s , or equivalently, we want our lattice points to lie in $\{\vec{x} \in \mathbb{R}^4 \mid \sum q_i x_i = s\}$. To capture all such integer points (and only these integer points), we consider the rational polytope Q defined by the convex hull

$$Q = \text{conv}\{(s/q_1, \dots, 0), \dots, (0, \dots, s/q_n)\}.$$

Generally, Q is not integral. Thus, we need only consider the integral polytope Δ defined as the convex hull of all integral points of Q , hereafter referred to as the *Newton polytope*.

Associated to Δ is a toric variety \mathbb{P}_Δ . The equations describing a family of hypersurfaces lying in \mathbb{P}_Δ are obtained from the Laurent polynomials $\sum_j \lambda_j \bar{x}^{\vec{p}_j}$ (see [11]). Here \vec{p}_j are the integral points of Δ , and as the λ_j vary we obtain different hypersurfaces in the family.

Computationally, it is useful to observe that the condition $\sum q_i x_i = s$ means that the rational polytope Q lies in a hyperplane of \mathbb{R}^4 . Using this condition, we may consider Q as lying in \mathbb{R}^3 and do the convex hull computations accordingly. (Several algorithms exist for taking convex hulls; details of this computation for the ‘‘Famous 95’’ may be found in [3].)

Now recall that for any K3 surface S ,

$$H^2(S, \mathbb{Z}) \cong (E_8)^2 \perp (U)^3 \text{ [2, p.241]}$$

where U is the hyperbolic plane $\begin{pmatrix} 0 & 1 \\ 1 & 0 \end{pmatrix} \sim \begin{pmatrix} -2 & 1 \\ 1 & 0 \end{pmatrix}$. We consider the intersection form on $H^2(S, \mathbb{Z})$, which gives us the bilinear form on the lattice.

The group of linear equivalence classes of Cartier divisors, denoted $\text{Pic}(S)$, injects into $H^2(S, \mathbb{Z})$ for K3 surfaces [2, p.241]. The image of $\text{Pic}(S)$ in $H^2(S, \mathbb{Z})$ (equal to $H^2(X, \mathbb{Z}) \cap H^{1,1}(X, \mathbb{C})$) is the algebraic cycles in $H^2(S, \mathbb{Z})$; this has no torsion, so we may consider $\text{Pic}(S)$ as a

lattice, and call it the Picard lattice. For ease of discussion, Section 2 reviews the lattice theory used later in the paper.

Computation of $\text{Pic}(S)$ is nontrivial. We are able to accomplish it for the generic members of the “Famous 95” families because of the fortunate conjunction of two properties: (1) they are hypersurfaces in special weighted projective spaces, so we can determine the rank of $\text{Pic}(S)$ (see Section 3), and (2) they are nondegenerate hypersurfaces in toric varieties, so we can easily and explicitly desingularize them (see Section 4.1). We will generally refer to the singular model as \bar{S} and the smooth model as S . Our method of computing $\text{Pic}(S)$ is roughly as follows: After determining $\rho(S)$, the rank of $\text{Pic}(S)$, we apply toric techniques to desingularize \bar{S} . We use the nonsingular model with $\rho(S)$ to exhibit an elliptic fibration. (All K3 surfaces with $\rho(S) > 5$ are also elliptic surfaces, and most singular K3 2-dimensional toric hypersurfaces will fall into this category or have singularities whose exceptional curves form elliptic fibres.) Section 4 explains this process and contains theorems on the existence of elliptic fibrations. Finally, we analyze the elliptic fibration to produce $\text{Pic}(S)$. We introduce a number of techniques for analyzing a fibration in Section 5.

We end the paper with the application of these computations to mirror symmetry, in Section 6. Table 3 lists $\text{Pic}(S)$ for each of the “Famous 95” as well as the mirror lattice and corresponding family, if any. They are indexed by number as identified in [17].

2. SOME LATTICE THEORY

This section summarizes general background on lattices. Further information may be found in [15].

Definition 2.1. A lattice is a pair (L, b) where L is a finite-rank free \mathbb{Z} -module and b is a \mathbb{Z} -valued nondegenerate symmetric bilinear form on L .

We will only consider even lattices, i.e. those where $b(l, l)$ is even for all l . We also denote $b(l, l)$ by $\langle l, l \rangle$.

Definition 2.2. The *discriminant* of a lattice is the determinant of the matrix of the associated bilinear form.

2.1. Nikulin’s results. Lattices are classified by their discriminant quadratic forms q_L (often referred to simply as q). The discriminant form is defined on the discriminant group $G_L = L^*/L$, where $L^* = \text{Hom}(L, \mathbb{Z})$. We define q by $q_L(x) = \langle x, x \rangle \bmod 2\mathbb{Z}$, where $x \in G_L$; note that q is the quadratic form associated to the bilinear form b which defines the lattice L . We will define three classes of forms on

G_L : $w_{p,k}^\epsilon, u_k, v_k$. An excellent explanation of these forms can be found in [4].

Definition 2.3. The quadratic form $w_{p,k}^\epsilon$ on \mathbb{Z}_{p^k} is defined in cases, depending on the value of p .

Case 1. For $p \neq 2$, $\epsilon \in \{\pm 1\}$. The form has generator value $q(1) = ap^{-k} \pmod{2\mathbb{Z}}$. For $\epsilon = 1$ we choose a to be the smallest positive even number with a quadratic residue; for $\epsilon = -1$ we choose a to be the smallest positive even number without a quadratic residue.

Case 2. For $p = 2$, there are more possibilities. For $k = 1, \epsilon \in \{\pm 1\}$, $w_{2,1}^\epsilon$ is defined as the form with generator value $q(1) = \epsilon/2$. For $k \geq 1$ and $\epsilon \in \{\pm 1, \pm 5\}$, $w_{2,k}^\epsilon$ is defined as the form with generator value $q(1) = \epsilon/2^k$.

Definition 2.4. The forms u_k, v_k on $\mathbb{Z}_{2^k} \oplus \mathbb{Z}_{2^k}$ are defined via their matrices, which are

$$u_k = 2^{-k} \begin{pmatrix} 0 & 1 \\ 1 & 0 \end{pmatrix} \quad v_k = 2^{-k} \begin{pmatrix} 2 & 1 \\ 1 & 2 \end{pmatrix}.$$

The following theorem is a combination of [15, 1.8.1, 1.8.2].

Theorem 2.5. (i) Every nontrivial, nondegenerate irreducible quadratic form on a finite abelian group is isomorphic to one of $u_k, v_k, w_{p,k}^\epsilon$.
(ii) Every nondegenerate quadratic form on a finite abelian group is isomorphic to an orthogonal direct sum of $u_k, v_k, w_{p,k}^\epsilon$.
(iii) This representation of a quadratic form is not unique.

2.2. Example: $T_{p,q,r}$ and $M_{\vec{p},\vec{r},k}$ Lattices. A $T_{p,q,r}$ lattice is so named because its graph forms the shape of a **T** (see Figure 1), where each vertex of the graph represents a (-2) -curve. In this notation, p, q , and r are the lengths of the three legs, counting the central vertex each time. The discriminant of a $T_{p,q,r}$ is $pqr - pq - pr - qr$ and its rank is $p+q+r-2$. Some of these lattices are isomorphic to Dynkin diagrams; for example, $T_{2,3,7}$ is $E_8 \perp U$. These lattices are well-known; they are carefully and clearly studied in [4].

A generalization of the $T_{p,q,r}$ lattices is

Definition 2.6. Let $\vec{p} = (p_1, \dots, p_n)$ be an n -tuple of positive integers, ordered from least to greatest. Let $\vec{i} = (i_1, \dots, i_n)$ be an n -tuple of integers such that $i_j \leq \lceil \frac{p_j}{2} \rceil$. Let $k \geq -4$ be an even integer. Then $M_{\vec{p},\vec{i},k}$ is the lattice defined by the incidence matrix of the following graph:

Begin with a central vertex c with self-intersection k . For each j , adjoin

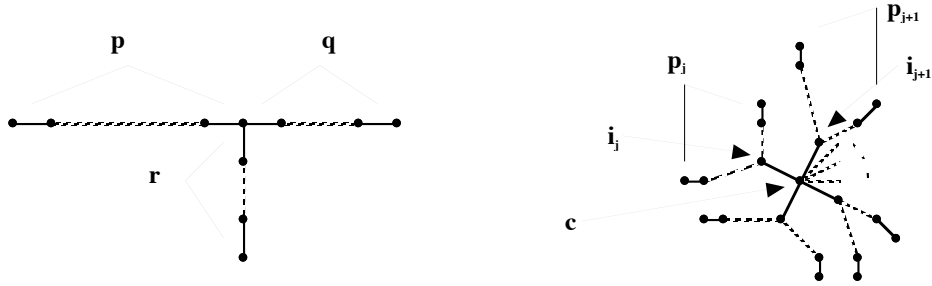


FIGURE 1. $T_{p,q,r}$ and $M_{\vec{p},\vec{r},k}$ graphs

to this vertex a Dynkin diagram of type A_{p_j} by adding an edge between c and vertex i_j of the Dynkin diagram. Note that every vertex, except possibly c , represents a (-2) -curve.

By taking the determinant of the associated matrix, Dolgachev has calculated the discriminant of an $M_{\vec{p},\vec{r},k}$; it is

$$\text{disc}(M_{\vec{p},\vec{r},k}) = -(-1)^{\sum_{j=1}^n p_j} (p_1 + 1) \dots (p_n + 1) \left(k + \sum_{j=1}^n \frac{i_j(p_j + 1 - i_j)}{p_j + 1} \right).$$

When $k = -2$, $n = 3$, $i_j = 1$, we have a $T_{p,q,r}$ lattice.

Note that there is no algorithm for computing the associated quadratic form to an $M_{\vec{p},\vec{r},k}$ (or even for a $T_{p,q,r}$ – see [4]).

3. CALCULATING $\rho(S)$

Henceforth in this paper, S will denote the generic member of one of the “Famous 95” families. We would like to determine $\rho(S)$, the rank of the Picard lattice. Let $\psi : S \rightarrow \bar{S}$ be the resolution of singularities. We know that \bar{S} has a natural desingularization in terms of A_{p_j} singularities (see Section 4.1). In this notation, the subscript refers to the Milnor number of the singularity.

Lemma 3.1. *Let \bar{S} be a generic surface in one of the 95 families. Then $\rho(\bar{S}) = 1$.*

Proof of 3.1. For each of the “Famous 95” families, the degree of the generic surface is $s = q_0 + q_1 + q_2 + q_3$ (again, by adjunction). In [5], the author examines the cup product $c : H^1(\bar{S}, T_{\bar{S}})_0 \times H^{2,0}(\bar{S}) \rightarrow H^{1,1}(\bar{S})$, where $H^1(\bar{S}, T_{\bar{S}})_0$ represents the variations in \bar{S} from varying the coefficients in its equation ($T_{\bar{S}}$ is the Zariski tangent space). He concludes that if this map is surjective, then for generic \bar{S} , $\text{rk}(\text{Pic}(\bar{S})) = 1$.

We will now show that this map is surjective when $\deg(\bar{S}) = s$. Denote by $R = \bigoplus R_j$ the Jacobian ring $\mathbb{C}[x_0, x_1, x_2, x_3]/\langle \partial f \rangle$, graded by degree. In [8, 4.3] the generators of $H_0^{2,0}(\bar{S})$ and $H_0^{1,1}(\bar{S})$ are computed. $H_0^{1,1}(\bar{S})$ is generated by the monomials m in R such that $(1/(\deg(\bar{S})))(((\deg_{x_0} m) + 1)q_0 + ((\deg_{x_1} m) + 1)q_1 + ((\deg_{x_2} m) + 1)q_2 + ((\deg_{x_3} m) + 1)q_3) = 2$. Because $\deg \bar{S} = q_0 + q_1 + q_2 + q_3$, this expression picks out monomials of total degree equal to $\deg(S) = s$. Thus, $H_0^{1,1}(\bar{S}) = R_s$. The same expression is used to find generators for $H_0^{2,0}(\bar{S})$, except that the expression is set equal to 1 and thus only the monomial 1, of total degree zero, generates $H_0^{2,0}(\bar{S})$ so that $H_0^{2,0}(\bar{S}) = R_0$. Now, by definition (see [2, p.31]), $H^1(\bar{S}, T_{\bar{S}})_0 = H^1(\bar{S}, \Omega_{\bar{S}})_0 = H_0^{1,1}(\bar{S})$ and so the map becomes $c : R_s \times H^{2,0}(\bar{S}) \rightarrow H^{1,1}(S)$. $H^2(\bar{S}, \mathbb{C}) = H^{2,0}(\bar{S}) \oplus H^{1,1}(\bar{S}) \oplus H^{0,2}(\bar{S})$ is torsion-free; therefore $H^{2,0}(\bar{S}) = R_0$ and $H^{1,1}(\bar{S}) = R_s$, so that we may interpret the map as $c : R_s \times R_0 \rightarrow R_s$. Because c is just the multiplication in R , it is an isomorphism as R_0 is generated by 1. Thus c is surjective, and for generic \bar{S} , $\text{rk}(\text{Pic}(\bar{S})) = 1$. \square

Lemma 3.2. *The contribution to $\text{Pic}(S)$ from desingularizing \bar{S} is $\sum_j p_j$.*

The proof of 3.2 is well-known and thus left to the reader.

Theorem 3.3. *Let S be the minimal nonsingular model of \bar{S} and p_j be the types of the A_{p_j} singularities of \bar{S} . Then $\rho(S) = 1 + \sum_j p_j$.*

Proof of 3.3. We combine 3.1 and 3.2 to obtain the result. \square

Remark. It is interesting to note that there are few results which compute the Picard number of the generic member of a family of toric hypersurfaces. If there were results for more general toric hypersurfaces, one could apply most of the techniques listed later to a wider class of objects.

4. FINDING $\text{PIC}(S)$ OVER \mathbb{Q}

4.1. Desingularization. To desingularize \bar{S} , we use the combinatorics of the Newton polytope Δ . Recall that singularities of \bar{S} are inherited from \mathbb{P}_{Δ} . We locate singularities of \mathbb{P}_{Δ} by examining the vertices and edges of Δ (see [12] and [9]). In fact, we may ignore vertices of Δ because \bar{S} does not intersect the corresponding torus orbits ([12]). To check whether an edge E_{ij} of Δ encodes a singularity, we look at the dual cone generated by vectors v_i, v_j normal to the incident faces F_i, F_j . (These vectors point to the corresponding vertices of the polar dual

polytope Δ° , which are integral for K3 toric hypersurfaces (see [1]).) The vectors v_i, v_j do not necessarily generate the lattice; we determine the number of curves added (n , as in A_n) by the number of additional vectors needed to generate the lattice (see [9], Ch. 2).

Additionally, each face of Δ corresponds to an irreducible curve; its genus is determined by the number of integer points on the face (see [11], [12]). The structure of Δ completely determines the intersections of the curves produced by desingularization and those which arise from faces of Δ . For example, any two faces F_i, F_j of Δ intersect in an edge E_{ij} of Δ . This corresponds geometrically to curves C_{F_i}, C_{F_j} ; their intersection number $C_{F_i} \cdot C_{F_j}$ is equal to the number of lattice points on E_{ij} , minus one. This follows from [9], Ch. 5. If there is a singularity at the intersection of C_{F_i} and C_{F_j} , then the intersection multiplicity gives the number of copies of the chain(s) of curves produced in resolving the singularities associated to E_{ij} .

We may use this information to create a graph, in which each curve is represented by a vertex and where intersections between curves are represented by edges. The intersection matrix of this graph (henceforth referred to as the *desingularization graph*) is a bilinear form, which is a lattice. This lattice is of the same rank as $\text{Pic}(S)$, generated by curves on the surface, and is certainly a sublattice of finite index of $\text{Pic}(S)$.

We now lay the groundwork for forming elliptic fibrations from the desingularization graph. Section 5 describes how to analyze these fibrations to obtain $\text{Pic}(S)$.

4.2. Forming Elliptic Fibrations.

Definition 4.1. An elliptic fibration is a regular map $\pi : S \rightarrow B$ from a surface S to some base curve B , such that the general fibre $\pi^{-1}(b)$ is an elliptic curve.

Because the surfaces we study are K3, the base curve is isomorphic to \mathbb{P}^1 . We only consider elliptic fibrations which have a finite number of sections; under this condition, all sections are torsion sections and are thus disjoint [14, Lemma, p.72]. There may be finitely many reducible fibres, and the possible types were listed by Kodaira [2, V.7].

Thus, we'll be looking for subgraphs in the desingularization graph which are isomorphic to graphs of fibres from the Kodaira Classification. Notice that because toric K3s only have A_n singularities, we are limited to fibres which are irreducible or which correspond to extended Dynkin diagrams.

Theorem 4.2. *If F is a configuration of curves on the K3 surface S , identical to one of Kodaira's list of elliptic fibres, then there exists an elliptic fibration $\pi : S \rightarrow \mathbb{P}^1$ with general fibre linearly equivalent to F .*

Proof. We see by using Riemann-Roch that $|F|$ has projective dimension 1; using an argument similar to [2, VIII.17.3], we can show it has empty base locus. Thus $|F|$ determines a map from S to \mathbb{P}^1 . Application of Bertini then shows that the generic element of $|F|$ is smooth. \square

In practice, we want to partition each output graph into collections of subgraphs corresponding to fibres, sections, and multisections. In this context, U is the intersection matrix of a section with an irreducible fibre. We begin by finding a fibre, then mark all adjacent vertices as sections/multisections, and partition the remaining subgraph into other fibres and sections/multisections if possible. However, sometimes we will be left with a collection of vertices which do not form any elliptic fibre.

Lemma 4.3. *Suppose on the K3 surface S there exists a fibration $\pi : S \rightarrow \mathbb{P}^1$ with exhibited fibre F . Then, if a collection of -2 curves disjoint from F corresponds to a proper subset of an extended Dynkin diagram, there exist curves sufficient to complete the fibre.*

The proof of Lemma 4.3 is left to the reader.

Note. In terms of partitioning output graphs, Lemma 4.3 allows us to add vertices to subgraphs to form extended Dynkin diagrams.

The effects of Lemma 4.3 can be seen in terms of linear algebra as well. For example, suppose the addition of only one curve is necessary to complete a fibre. The extended Dynkin diagrams have positive semidefinite forms, so the determinants of their intersection matrices are zero. The intersection matrix associated to an incomplete fibre has nonzero determinant. When we complete the fibre by adding one curve, the rank of the associated matrix (and thus that of the fibration) does not increase because the determinant becomes zero.

If there is more than one way to complete a fibre with the same (minimal) number of curves, more information is necessary to decide which fibre exists. The discriminant of the original intersection matrix gives us a finite number of possibilities (see Section 5.3) for the discriminant of the fibration. Usually comparing the discriminant of the proposed fibration to that of the original matrix is sufficient to determine which fibre we have.

One of the most useful tools in analyzing possible elliptic fibrations is the Shioda-Tate formula.

Lemma 4.4 ([16]). *Let $f : S \rightarrow B$ be an elliptic fibration (with section) of a smooth surface S , and let ρ be the rank of $\text{Pic}(S)$. Then*

$$\rho = 2 + \sum_{F_i} ((\# \text{ components in } F_i) - 1) + \text{rk}(MW),$$

where $\text{rk}(MW)$ is the rank of the Mordell-Weil group of sections, and F_i ranges over all fibres (note that irreducible fibres will not contribute to the sum). The number 2 corresponds to the contribution from a section and an irreducible fibre.

Most of the time we will find a fibration which shows that $\text{rk}(MW) = 0$, i.e. MW is finite. When we have shown that $\text{rk}(MW) = 0$, we have also shown that our fibration generates a finite-index sublattice of $\text{Pic}(S)$ because the rank is the same as that of $\text{Pic}(S)$.

Furthermore, we have

Lemma 4.5.

$$|MW|^2 \text{disc}(\text{Pic}(S)) = \prod_{F_i} \text{disc}(F_i).$$

This follows from [16, Corollary 1.7].

If we know that MW is finite, we have additional information which gives us an upper and lower bound on $|MW|$ = the number of sections. Our lower bound is the number of sections we have exhibited in the fibration. The upper bound is given by the gcd of the orders of G_{F_i} , because the torsion subgroup of MW (which in our case equals MW) embeds in the discriminant group of each fibre [14, p.70]. Often the bounds on $|MW|$ and the use of Lemma 4.5 will be enough to tell us that MW is trivial (at which point we are done, as we have then shown that the index in $\text{Pic}(S) = 1$).

Example 4.6. Figure 2 shows the *Mathematica* output for surface family number 26. Vertex 2 came from a face with one interior point, and so is a curve of genus 1; by 4.2, it is the generic fibre for an elliptic fibration. We know from our desingularization calculations (Theorem 3.3, Section 4.1) that $\rho = 14$.

Because curves 4 and 8 each intersect curve 2 exactly once, they must be sections of the fibration. Curves 1, 5-7, 9-12 are disjoint from curve 2, and form the reducible fibre \tilde{E}_7 (see Figure 3). This reducible fibre also intersects each of curves 4 and 8 exactly once, as every section intersects each fibre once. Finally, using Theorem 4.3 we must complete the remaining labeled curves 13-17 into a fibre or fibres. We know that each of these must be part of a different reducible fibre because a section

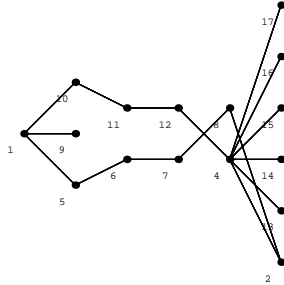


FIGURE
2. *Mathematica*
output

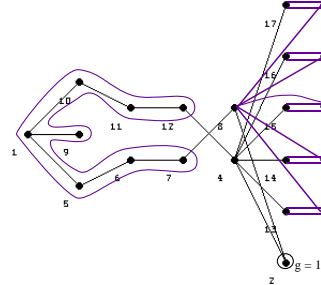


FIGURE
3. Complete
Fibration

intersects each fibre with multiplicity one, and section 4 intersects each of these curves with multiplicity one. The only fibre which conforms to these constraints is \tilde{A}_1 . Furthermore, we can only choose \tilde{A}_1 or we will violate the Shioda-Tate formula. Therefore, we add five vertices to the graph (see Figure 3).

The application of Shioda-Tate in this case gives us $14 = 2 + 7 + 5 \cdot 1 + \text{rk}(MW) = 14 + \text{rk}(MW)$ so $\text{rk}(MW) = 0$.

Notice that because section 8 must intersect each fibre once, and it does not naturally intersect any of curves 13-17, it must intersect each of the added curves.

5. ANALYZING FIBRATIONS TO COMPUTE $\text{Pic}(S)$

5.1. “Obvious” Elliptic Fibrations.

5.1.1. *Elliptic Fibrations Begun with an Irreducible Fibre.* Figure 4 shows a fibration for number 65. We are given via our computer output that curve 3 has genus 1 and that $\rho = 18$. considering curve 3 as a fibre gives us curves 17 and 19 as sections and the remaining curves as \tilde{D}_{16} .

Because $2 + 16 = 18$, the Shioda-Tate formula is satisfied with $\text{rk}(MW) = 0$. We have exhibited two sections, and $G_{\tilde{D}_{16}} = \mathbb{Z}_2 \oplus \mathbb{Z}_2$, so $2 \leq |MW| \leq 4$. As $|MW|^2 \in \{4, 9, 16\}$, using 4.5 gives $|MW|^2 \text{disc}(\text{Pic}(S)) = 4$. Thus $|MW|^2 = 4$, so that $|MW| = 2$ and $\text{disc}(\text{Pic}(S)) = 1$. We notice immediately that therefore $\text{Pic}(S) \neq D_{16} \perp U$ because that lattice has discriminant 4. This indicates we might wish to look for another fibration, which leads us to...

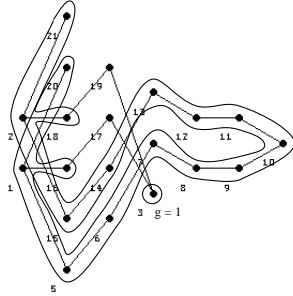


FIGURE
4. First
Fibration

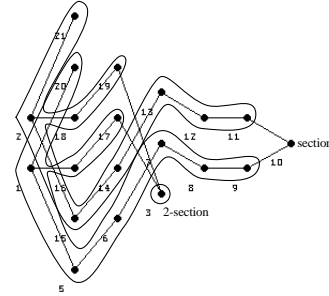


FIGURE
5. Second
Fibration

5.1.2. *Elliptic Fibrations with no Obvious Irreducible Fibre.* It happens frequently that we find more than one fibration. For example, in Figure 5 we see another elliptic fibration for number 65, namely $E_8 \perp E_8 \perp U$.

Application of Shioda-Tate shows that $\text{rk}(MW) = 0$, and formula 4.5 reads as $1 \cdot \text{disc}(\text{Pic}(S)) = 1$. Thus $\text{Pic}(S) = E_8 \perp E_8 \perp U$. Note that $D_{16} \perp U$ has index 2 in $E_8 \perp E_8 \perp U$. In 5.3, we will show more generally how to determine $\text{Pic}(S)$ when its discriminant does not match that of the fibration. In cases where different fibrations produce seemingly different $\text{Pic}(S)$, we reconcile the discrepancy using the isomorphism relations on the forms corresponding to the two lattices (see [4], [15]).

5.2. $T_{p,q,r}$ **Fibrations.** Sometimes we will not find any satisfactory fibrations using the Dynkin diagrams, but will find a $T_{p,q,r}$ lattice (defined in 2.2).

Example 5.1. Family number 4, which has $\rho = 10$, is shown in Figure 6. The lattice $T_{4,4,4}$ exhibited in Figure 6 has rank 10 as well. Because number 4 is one of Arnold's singularities, this is sufficient to compute $\text{Pic}(S) = T_{4,4,4}$, but for other cases we will need to use techniques from sections 5.3 and 5.5 to show that the $T_{p,q,r}$ lattice has index 1 in $\text{Pic}(S)$.

5.3. **Intermediate Lattice Calculations.** We will now resolve the uncertainties raised by the first fibration (Figure 4) for number 65. More generally, we use intermediate lattice calculations when we have exhibited more than one section, especially when the number of exhibited sections divides $\prod_{F_i} \text{disc}(F_i)$. First, recall that because we've found a lattice of the correct rank, it must embed in $\text{Pic}(S)$ with finite index. If L is the lattice corresponding to our fibration, then $L \subseteq \text{Pic}(S) \subseteq L^*$

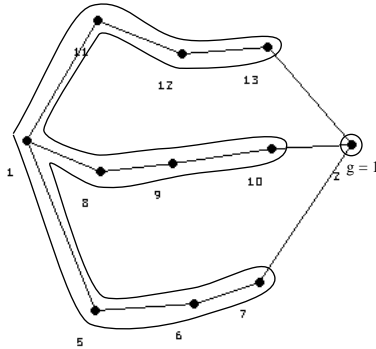


FIGURE 6. Number 4

(see Section 2.1 for notation). Additionally, there is a 1-1 correspondence between the possible “intermediate lattices” M and q -isotropic subgroups H of the discriminant group G_L [15, 1.4.1(a)].

In fact, there is a constructive method for listing the different possibilities for $\text{Pic}(S)$ via a formula of Nikulin:

Theorem 5.2 ([15]). *For each q_L -isotropic subgroup H of G_L , $q_M = (q_L|H^\perp)/H$.*

Let us interpret this statement via an example.

Example 5.3. Number 26 (see Figure 7).

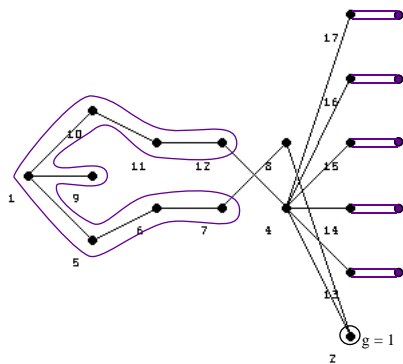


FIGURE 7. Number 26

Step 1. Find all q_L -isotropic subgroups of G_L . A subgroup is isotropic if every element of the subgroup has value q_L -value $0 \pmod{2\mathbb{Z}}$.

a	$a+(1,1,1,1)$	$q(a) - q(a+(1,1,1,1))$
$(0,0,0,0)$	$(1,1,1,1)$	$0 - 0 = 0$
$(0,0,0,1)$	$(1,1,1,0)$	$(-1/2) - (-3/2) = 1$
$(0,0,1,1)$	$(1,1,0,0)$	$(-1) - (-1) = 0$
$(0,1,1,1)$	$(1,0,0,0)$	$(-3/2) - (-1/2) = -1$
$(1,1,1,1)$	$(0,0,0,0)$	$0 - 0 = 0$

TABLE 1. Calculation of H^\perp for Number 26

For number 26, we have $\tilde{E}_7 + 5\tilde{A}_1$. Each of these degenerate fibres has discriminant group \mathbb{Z}_2 , so $G_L \cong (\mathbb{Z}_2)^6$. The form corresponding to E_7 is $w_{2,1}^1$ and the value on the generator is $1/2$. The form corresponding to A_1 is $w_{2,1}^{-1}$ and the value on the generator is $-1/2$. These forms are independent, so in evaluating them on $(\mathbb{Z}_2)^6$ we can just add the values on the components. Immediate examples of q_L -isotropic subgroups are those generated by $(1,0,0,0,0,1)$, $(1,0,0,0,1,0)$, $(1,0,0,1,0,0)$, $(1,0,1,0,0,0)$, and $(1,1,0,0,0,0)$. Fortunately, we also know that

Theorem 5.4 ([15]). *Two intermediate lattices M_1, M_2 are isomorphic if and only if the corresponding q_L -isotropic subgroups H_1, H_2 of G_L are conjugate under an automorphism of L .*

Remark. This corresponds, for example, to permuting several copies of some Dynkin diagram, or equivalently to permuting the relevant coordinates of several copies of some quadratic form.

So in our example, all five of the q_L -isotropic subgroups listed above can be represented without redundancy by $(1,1,0,0,0,0)$. In similar fashion, we have two other distinct isotropic subgroups represented by $(0,0,1,1,1,1)$ and $(1,1,1,1,1,1)$.

Step 2. Determine H^\perp .

To simplify the example, we will only compute for $H = (0,0,1,1,1,1)$. Up to permutation of the entries, we really only have 5 elements to deal with: $(0,0,0,0,0,0)$, $(0,0,0,0,0,1)$, $(0,0,0,0,1,1)$, $(0,0,0,1,1,1)$, $(0,0,1,1,1,1)$. We will suppress the first 2 entries as they are always 0. Now we determine which of these are perpendicular to $H = \langle(1,1,1,1)\rangle$ with respect to the quadratic form. This holds true for an element a when $q(a) - q(a+(1,1,1,1)) = 0$.

So respectively, for these 5 types of elements, we have the data in Table 1.

elt	elt + (1,1,1,1)	q_L value
(0,0,0,0)	(1,1,1,1)	0
(0,0,1,1)	(1,1,0,0)	-1
(0,1,0,1)	(1,0,1,0)	-1
(0,1,1,0)	(1,0,0,1)	-1

TABLE 2. Values of the form q_M corresponding to H for Number 26

Step 3. List all elements in H^\perp and their values on q_L . Group them by conjugacy class in order to mod out by H . Using this list of values, determine the form of the intermediate lattice corresponding to H .

Table 2 lists all elements of $H = \langle (1,1,1,1) \rangle$ by conjugacy class, and their q_L -values.

This data corresponds to the form v . We must also retain the original form on the first two copies of \mathbb{Z}_2 ($w_{2,1}^{-1} \perp w_{2,1}^1$) because they were not involved in the calculation; they correspond to the zero-entries we suppressed above.

We have only computed q_M for one of the three distinct q_L -isotropic subgroups. Number 26 is very illustrative in that the other two intermediate lattices are $(w_{2,1}^{-1})^4$ and $u \perp v$, neither of which is isomorphic to $v \perp w_{2,1}^{-1} \perp w_{2,1}^1$. This creates another question: which one is correct? We need to look on the desingularization graph for other fibrations which confirm that one of these choices is correct and that the others are not possible. (It turns out that only $u \perp v$ is possible; see [3, p.80].)

Those hypersurface families for which we used intermediate lattice calculations are 15, 16, 23, 26, 29, 30, 32, 34, 35, 46, 52, 54 - 56, 65, 68, 73 - 76, 80, 83, 84, 86, 92; details are in [3].

5.4. Methods for Fibrations Without Sections. Sometimes we'll only be able to find a fibration which has only multisections, and no sections.

Theorem 5.5 ([10]). *Let $\pi : S \rightarrow B$ be an elliptic fibration. Then there exists a fibration $j : \mathbf{J}_\pi(S) \rightarrow B$ with the following properties:*

- $j : \mathbf{J}_\pi(S) \rightarrow B$ has a section
- each fibre of π is isomorphic to some fibre of j
- if π has a section, then $\mathbf{J}_\pi(S) \cong S$.

We refer to $j : \mathbf{J}_\pi(S) \rightarrow B$ in Theorem 5.5 as the *Jacobian fibration*. One way to construct $\mathbf{J}_\pi(S)$ from S is to take the Jacobian variety of the generic fibre S_η and realize this as the generic fibre of some elliptic surface which has a section. By Theorem 5.5, the fibres of the Jacobian

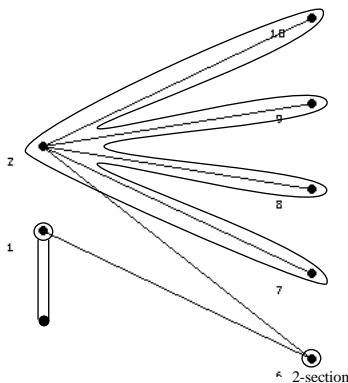


FIGURE 8. Fibration for Number 19

fibration are the same as those of the non-Jacobian fibration; likewise, $\rho(S) = \rho(\mathbf{J}_\pi(S))$.

Example 5.6. In number 19 (Figure 8) we immediately see that curves 2, 7-10 form a \tilde{D}_4 . Thus curve 6 is a 2-section and we can add a curve, intersecting curve 1 twice, to form an \tilde{A}_1 .

We can show that this must be a non-Jacobian fibration using direct computations on the intersection matrix. (In practice, we show by trial and error that if a section existed for the fibration, then the rank of the intersection matrix would exceed ρ .) For our example, number 19, there is no fibration in which one can exhibit a section and satisfy Shioda-Tate with $\text{rk}(MW) = 0$. However, the Jacobian fibration associated to Figure 8 satisfies Shioda-Tate with $\text{rk}(MW) = 0$; $\rho = 7$ so we have $7 = 2 + 4 + 1$.

In other words, a non-Jacobian fibration gives us information about $\text{Pic}(\mathbf{J}(S))$ and what we now need to know is the relationship between $\text{Pic}(S)$ and $\text{Pic}(\mathbf{J}(S))$.

We have shown ([3]) that there exists a map

$$\phi : \text{Pic}(S) \hookrightarrow \text{Pic}(\mathbf{J}(S))$$

of finite index n , where n is the index of multisections (the gcd of degrees of multisections). As $\text{Pic}(\mathbf{J}(S))$ is easy to compute, this map along with application of lattice theory completely determine $\text{Pic}(S)$. The current proof of existence uses moduli spaces of sheaves; we are convinced that there is a more direct proof and are working to complete one. This map was used to calculate $\text{Pic}(S)$ in the nine cases for which we exhibited non-Jacobian fibrations (numbers 2, 6, 18, 19, 31, 33, 53, 62, 69; details in [3]). In each case, we showed that the existence of a section increases the Picard number.

5.5. Calculating $\text{Pic}(S)$ from the Intersection Matrix. The intersection matrix for each desingularization graph represents a quadratic form, which is calculable. This is particularly useful when we cannot find a suitable fibration, or when we cannot show that MW is finite. Because the intersection matrix has rank equal to $\rho(S)$, it is of finite index in $\text{Pic}(S)$. Thus, if the discriminant of the matrix is square-free, the index is 1 and we need merely determine the corresponding form. (This was true for every case where MW was of indeterminate rank.) If the discriminant is not square-free, then there are a finite number of possibilities for $\text{Pic}(S)$ as per Section 5.3.

Note. The matrices have dimension $(\rho + 3) \times (\rho + 3)$, and rank ρ , so to determine the discriminant of such a matrix we must find the minimum value of the determinants of the $\rho \times \rho$ minors.

It should be mentioned that there is no general algorithm for determining the quadratic form which corresponds to a matrix. One must decide based on the values of the form on its generators and on the relations between these generators. Those surfaces for which we computed $\text{Pic}(S)$ from the matrix are 3, 7, 8, 17, 21, 36, 63, 66, 89, 94, 95; details are in [3].

6. TABLE OF PICARD LATTICES AND APPLICATION TO MIRROR SYMMETRY

Before presenting the available data on the “Famous 95,” we briefly describe the original motivation for our work.

The 14 Arnold singularities occur on Reid’s “Famous 95” list. It is described completely in [7] that the “strange duality” of Dolgachev and Gabrielov for the 14 Arnold singularities is a K3 analogue to the more recently studied Calabi-Yau threefold mirror symmetry. The question arises: Can one find a larger class of surfaces which mirror each other? The “Famous 95” are a natural set of K3 surfaces to investigate, as they arise so often; Dolgachev remarked in [7] that it would be most interesting to see if all surfaces on the list mirror each other. (Surprisingly, they do not.¹)

Definition 6.1. Two K3 surfaces form a mirror pair (S, \check{S}) if

$$\text{Pic}(S)_{H^2(S, \mathbb{Z})}^\perp = \text{Pic}(\check{S}) \perp U \text{ as lattices.}$$

¹While Batyrev’s mirror construction does not always give the correct K3 mirror (see [7]), the spirit of his work suggests that Kreuzer/Skarke’s 4319 toric K3 hypersurfaces [13] will mirror each other; the author is currently working to confirm this.

We refer to $\text{Pic}(\check{S})$ as the mirror lattice; to compute $\text{Pic}(\check{S})$, we use the fact that $L_{H^2(S,\mathbb{Z})}^\perp = M$ if and only if $q_L = -q_M$ [15, 1.6.2].

By computing $\text{Pic}(S)$ for each of the ‘‘Famous 95’’, we can see which families mirror each other, and that the list is not self-mirroring. The following table summarizes this data. The ‘‘No.’’ column indexes the surfaces as in [17], as does the ‘‘Mirror Family’’ column, and the ‘‘Weights’’ column gives the weights of the projective variables in the corresponding weighted projective space. As for the notation in the $\text{Pic}(S)$ and ‘‘Mirror Lattice’’ columns, the lattices A_n, D_n, E_n are the standard Dynkin lattices; U is the hyperbolic plane (see Section 1); the forms u, v , and $w_{p,k}^\epsilon$ are defined in Section 2.1; and, $T_{p,q,r}$ and $M_{\vec{p},\vec{r},k}$ are defined in Section 2.2. Complete details of each calculation are in [3] and available from the author.

TABLE 3. $\text{Pic}(S)$ for the 95 Families and Their Mirrors

No.	Rank	$\text{Pic}(S)$	Mirror Lattice and Family	Weights	
1	$\rho = 1$	$\langle 4 \rangle$	$(E_8)^2 \perp \langle -4 \rangle \perp U$	56, 73	(1, 1, 1, 1)
2	$\rho = 12$	$E_6 \perp D_4 \perp U(3)$	$D_4 \perp A_2 \perp U(3)$	not on list	(2, 3, 3, 4)
3	$\rho = 4$	$M_{(1,1,1),(1,1,1),0}$	$E_8 \perp D_4 \perp A_2 \perp U$	not on list	(1, 1, 2, 2)
4	$\rho = 10$	$T_{4,4,4}$	$T_{4,4,4}$	4	(1, 3, 4, 4)
5	$\rho = 1$	$\langle 2 \rangle$	$(E_8)^2 \perp A_1 \perp U$	52, tetra.	(1, 1, 1, 3)
6	$\rho = 6$	$D_4 \perp U(2)$	$D_8 \perp D_4 \perp U$	26, 34, 76	(1, 2, 2, 5)
7	$\rho = 3$	$M_{(1,1),(1,1),0}$	$E_8 \perp D_7 \perp U$	64	(1, 1, 2, 4)
8	$\rho = 7$	$M_{(1,1,2,2),(1,1,1,1),-2}$	$q = w_{3,1}^1 \perp w_{2,2}^{-1}$	not on list	(1, 2, 3, 6)
9	$\rho = 10$	$T_{2,5,5}$	$T_{2,5,5}$	9,71	(1, 4, 5, 10)
10	$\rho = 2$	U	$(E_8)^2 \perp U$	65, 46, 80	(1, 1, 4, 6)
11	$\rho = 12$	$E_6 \perp D_4 \perp U$	$D_4 \perp A_2 \perp U$	24	(2, 3, 10, 15)
12	$\rho = 6$	$D_4 \perp U$	$E_8 \perp D_4 \perp U$	27, 49	(1, 2, 9, 6)
13	$\rho = 8$	$E_6 \perp U$	$E_8 \perp A_2 \perp U$	20, 59	(1, 3, 8, 12)
14	$\rho = 10$	$E_8 \perp U$	$E_8 \perp U$	14,28,45,51	(1, 6, 14, 21)
15	$\rho = 14$	$E_6 \perp (A_2)^3 \perp U$	$(A_2)^2 \perp U(3)$	not on list	(3, 3, 4, 5)
16	$\rho = 16$	$E_8 \perp (A_2)^3 \perp U$	$A_2 \perp U(3)$	not on list	(3, 6, 7, 8)
17	$\rho = 14$	$T_{2,5,5} \perp A_4$	$A_4 \perp \begin{pmatrix} 2 & 1 \\ 1 & -2 \end{pmatrix}$	not on list	(2, 3, 5, 5)

continued on next page

continued from previous page

No.	Rank	Pic(S)	Mirror Lattice and Family	Weights
18	$\rho = 8$	$M_{(1,2,2,2),(1,1,1,1),-2}$	$q = w_{3,2}^1 \perp w_{3,1}^1$	not on list (1, 2, 3, 3)
19	$\rho = 7$	$M_{(1,1,1,1,2), (1,1,1,1,1),-2}$	$q = v \perp w_{2,3}^1$	not on list (1, 2, 2, 3)
20	$\rho = 12$	$E_8 \perp A_2 \perp U$	$E_6 \perp U$	13, 72 (1, 6, 8, 9)
21	$\rho = 2$	$\begin{pmatrix} 2 & 1 \\ 1 & -2 \end{pmatrix}$	$E_8 \perp T_{2,5,5}$	30, 86 (1, 1, 1, 2)
22	$\rho = 10$	$E_6 \perp A_2 \perp U$	$E_6 \perp A_2 \perp U$	22 (1, 3, 5, 6)
23	$\rho = 11$	$D_5 \perp D_4 \perp U(2)$	$D_4 \perp A_3 \perp U(2)$	not on list (2, 2, 3, 5)
24	$\rho = 8$	$D_4 \perp A_2 \perp U$	$E_6 \perp D_4 \perp U$	11 (1, 2, 4, 5)
25	$\rho = 4$	$A_2 \perp U$	$E_8 \perp E_6 \perp U$	43, 48, 88 (1, 1, 3, 4)
26	$\rho = 14$	$D_8 \perp D_4 \perp U$	$D_4 \perp U(2)$	6 (2, 4, 5, 9)
27	$\rho = 14$	$E_8 \perp D_4 \perp U$	$D_4 \perp U$	12 (2, 3, 8, 11)
28	$\rho = 10$	$E_8 \perp U$	$E_8 \perp U$	14, 28, 45, 51 (1, 3, 7, 10)
29	$\rho = 16$	$T_{2,5,5} \perp D_6$	$q = w_{5,1}^{-1} \perp (w_{2,1}^{-1})^2$	not on list (4, 5, 6, 15)
30	$\rho = 18$	$E_8 \perp T_{2,5,5}$	$\begin{pmatrix} 2 & 1 \\ 1 & -2 \end{pmatrix}$	21 (5, 7, 8, 20)
31	$\rho = 15$	$E_6 \perp A_7 \perp U$	$q = w_{2,3}^{-1} \perp w_{3,1}^1$	not on list (3, 4, 5, 12)
32	$\rho = 10$	$D_4 \perp D_4 \perp U(2)$	$D_4 \perp D_4 \perp U(2)$	32 (2, 2, 3, 7)
33	$\rho = 12$	$M_{(1,1,1,1,2,2,3), (1,1,1,1,1,1,1),-4}$	$q = w_{3,1}^1 \perp v \perp w_{2,1}^1 \perp w_{2,1}^{-1}$	not on list (2, 3, 4, 9)
34	$\rho = 14$	$D_8 \perp D_4 \perp U$	$D_4 \perp U(2)$	6 (2, 6, 7, 15)
35	$\rho = 16$	$E_8 \perp A_6 \perp U$	$M_{(1,2),(1,1),0}$	66 (3, 4, 7, 14)
36	$\rho = 13$	$T_{2,5,5} \perp A_3$	$D_5 \perp \begin{pmatrix} 2 & 1 \\ 1 & -2 \end{pmatrix}$	not on list (2, 3, 5, 10)
37	$\rho = 9$	$T_{3,4,4}$	$T_{2,5,6}$	58 (1, 3, 4, 8)
38	$\rho = 11$	$E_8 \perp A_1 \perp U$	$E_7 \perp U$	50, 82 (1, 6, 8, 15)
39	$\rho = 9$	$E_6 \perp A_1 \perp U$	$E_7 \perp A_2 \perp U$	60 (1, 3, 5, 9)
40	$\rho = 7$	$D_4 \perp A_1 \perp U$	$E_7 \perp D_4 \perp U$	81 (1, 2, 4, 7)
41	$\rho = 13$	$E_6 \perp D_5 \perp U$	$A_3 \perp A_2 \perp U$	not on list (2, 3, 7, 12)
42	$\rho = 3$	$A_1 \perp U$	$E_8 \perp E_7 \perp U$	68, 83, 92 (1, 1, 3, 5)
43	$\rho = 16$	$E_8 \perp E_6 \perp U$	$A_2 \perp U$	25 (3, 4, 11, 18)

continued on next page

continued from previous page

No.	Rank	Pic(S)	Mirror Lattice and Family	Weights	
44	$\rho = 7$	$D_5 \perp U$	$E_8 \perp A_3 \perp U$	not on list	(1, 2, 5, 8)
45	$\rho = 10$	$E_8 \perp U$	$E_8 \perp U$	14,28,45,51	(1, 4, 9, 14)
46	$\rho = 18$	$E_8^2 \perp U$	U	10	(5, 6, 22, 33)
47	$\rho = 15$	$E_7 \perp E_6 \perp U$	$A_2 \perp A_1 \perp U$	not on list	(3, 4, 14, 21)
48	$\rho = 16$	$E_8 \perp E_6 \perp U$	$A_2 \perp U$	25	(3, 5, 16, 24)
49	$\rho = 14$	$E_8 \perp D_4 \perp U$	$D_4 \perp U$	12	(2, 5, 14, 21)
50	$\rho = 9$	$E_7 \perp U$	$E_8 \perp A_1 \perp U$	38, 77	(1, 4, 10, 15)
51	$\rho = 10$	$E_8 \perp U$	$E_8 \perp U$	14,28,45,51	(1, 5, 12, 18)
52	$\rho = 19$	$E_8 \perp D_9 \perp U \cong$ $(E_8)^2 \perp \langle -4 \rangle \perp$ U	$\langle 4 \rangle, q = w_{2,2}^1$	5	(7, 8, 9, 12)
53	$\rho = 15$	$M_{(1,2,2,2,3,4),}$ $(1,1,1,1,1,1), -4$	$q = w_{3,2}^1 \perp$ $w_{3,1}^1 \perp w_{2,1}^{-1}$	not on list	(3, 4, 5, 6)
54	$\rho = 16$	$E_8 \perp (A_2)^3 \perp U$	$A_2 \perp U(3)$	not on list	(3, 5, 6, 7)
55	$\rho = 15$	$D_9 \perp D_4 \perp U$	$w_{2,2}^1 \perp u$	not on list	(2, 5, 6, 7)
56	$\rho = 19$	$E_8^2 \perp A_1 \perp U$	$\langle 2 \rangle, q = w_{2,1}^1$	1	(5, 6, 8, 11)
57	$\rho = 17$	$E_8 \perp D_5 \perp$ $A_2 \perp U$	$w_{2,2}^5 \perp w_{3,1}^{-1}$	not on list	(4, 5, 6, 9)
58	$\rho = 11$	$T_{2,5,6}$	$T_{3,4,4}$	37	(1, 4, 5, 6)
59	$\rho = 12$	$E_8 \perp A_2 \perp U$	$E_6 \perp U$	13, 72	(1, 5, 7, 8)
60	$\rho = 11$	$E_7 \perp A_2 \perp U$	$E_6 \perp A_1 \perp U$	39	(1, 4, 6, 7)
61	$\rho = 18$	$E_8 \perp D_8 \perp U$	$U(2)$	not on list	(4, 6, 7, 11)
62	$\rho = 16$	$D_9 \perp D_5 \perp U$	$q = w_{2,2}^1 \perp w_{2,2}^5$	not on list	(3, 4, 5, 8)
63	$\rho = 8$	$M_{(1,1,2,3),(1,1,1,1),-2}$	$T_{2,5,5} \perp (A_1)^2$	not on list	(1, 2, 3, 4)
64	$\rho = 17$	$E_8 \perp D_7 \perp U$	$M_{(1,1),(1,1),0}$	7	(3, 4, 7, 10)
65	$\rho = 18$	$E_8^2 \perp U$	U	10	(3, 5, 11, 14)
66	$\rho = 4$	$M_{(1,2),(1,1),0}$	$E_8 \perp A_6 \perp U$	35	(1, 1, 2, 3)
67	$\rho = 14$	$E_6^2 \perp U \cong E_8 \perp$ $(A_2)^2 \perp U$	$(A_2)^2 \perp U$	not on list	(2, 3, 7, 9)
68	$\rho = 17$	$E_8 \perp E_7 \perp U$	$A_1 \perp U$	42	(3, 4, 10, 13)
69	$\rho = 13$	$D_4 \perp A_7 \perp U$	$q = w_{2,3}^{-1} \perp v$	not on list	(2, 3, 4, 7)
70	$\rho = 14$	$E_8 \perp A_2 \perp$ $(A_1)^2 \perp U$	$q = w_{3,1}^{-1} \perp$ $(w_{2,1}^1)^2$	not on list	(2, 3, 5, 8)

continued on next page

<i>continued from previous page</i>					
No.	Rank	Pic(S)	Mirror Lattice and Family		Weights
71	$\rho = 10$	$T_{2,5,5}$	$T_{2,5,5}$	9, 71	(1, 3, 4, 7)
72	$\rho = 8$	$E_6 \perp U$	$E_8 \perp A_2 \perp U$	20, 59	(1, 2, 5, 7)
73	$\rho = 19$	$E_8^2 \perp A_1 \perp U$	$\langle 2 \rangle, q = w_{2,1}^1$	1	(7, 8, 10, 25)
74	$\rho = 17$	$M_{(3,3,4,6),(1,1,1,3),-4}$	$q = w_{2,3}^{-5}$	not on list	(4, 5, 7, 16)
75	$\rho = 13$	$E_7 \perp (A_1)^4 \perp U$	$(A_1)^5 \perp U$	not on list	(2, 4, 5, 11)
76	$\rho = 14$	$D_8 \perp D_4 \perp U$	$D_4 \perp U(2)$	6	(2, 5, 6, 13)
77	$\rho = 11$	$E_8 \perp A_1 \perp U$	$E_7 \perp U$	50, 82	(1, 5, 7, 13)
78	$\rho = 10$	$E_7 \perp A_1 \perp U$	$E_7 \perp A_1 \perp U$	78	(1, 4, 6, 11)
79	$\rho = 15$	$E_8 \perp D_5 \perp U$	$A_3 \perp U$	not on list	(2, 5, 9, 16)
80	$\rho = 18$	$E_8^2 \perp U$	U	10	(4, 5, 13, 22)
81	$\rho = 13$	$E_8 \perp (A_1)^3 \perp U$	$D_4 \perp A_1 \perp U$	40	(2, 3, 8, 13)
82	$\rho = 9$	$E_7 \perp U$	$E_8 \perp A_1 \perp U$	38, 77	(1, 3, 7, 11)
83	$\rho = 17$	$E_8 \perp E_7 \perp U$	$A_1 \perp U$	42	(4, 5, 18, 27)
84	$\rho = 18$	$E_8 \perp A_8 \perp U$	$q = w_{3,2}^{-1}$	not on list	(5, 6, 7, 9)
85	$\rho = 13$	$D_4 \perp A_6 \perp$ $A_1 \perp U$	$D_4 \perp \langle 14 \rangle \perp U$	not on list	(2, 3, 4, 5)
86	$\rho = 18$	$E_8 \perp T_{2,5,5}$	$\begin{pmatrix} 2 & 1 \\ 1 & -2 \end{pmatrix}$	21	(4, 5, 7, 9)
87	$\rho = 10$	$T_{3,4,5}$	$T_{3,4,5}$	87	(1, 3, 4, 5)
88	$\rho = 16$	$E_8 \perp E_6 \perp U$	$A_2 \perp U$	not on list	(2, 5, 9, 11)
89	$\rho = 8$	$M_{(1,2,4),(1,1,2),-2}$	$A_{10} \perp U$	not on list	(1, 2, 3, 5)
90	$\rho = 17$	$E_8 \perp D_6 \perp$ $A_1 \perp U$	$A_1 \perp U(2)$	not on list	(4, 6, 7, 17)
91	$\rho = 18$	$E_8 \perp E_7 \perp A_1 \perp$ U	$q = w_{2,1}^1 \perp w_{2,1}^{-1}$	not on list	(5, 6, 8, 19)
92	$\rho = 17$	$E_8 \perp E_7 \perp U$	$A_1 \perp U$	42	(3, 5, 11, 19)
93	$\rho = 16$	$E_8 \perp D_6 \perp U$	$(A_1)^2 \perp U$	not on list	(3, 4, 10, 17)
94	$\rho = 16$	$M_{(2,3,4,6),(1,1,2,2),-4}$	$q = w_{19,1}^1$	not on list	(3, 4, 5, 7)
95	$\rho = 14$	$M_{(1,2,4,6),(1,1,2,3),-4}$	$q = w_{17,1}^{-1}$	not on list	(2, 3, 5, 7)

ACKNOWLEDGEMENTS

The author is grateful to I. Dolgachev for supervising this work, which was part of her Ph.D. dissertation at the University of Michigan. She would also like to thank W. Cherry for general consultations, J.H. Keum for pointing out an omission in a previous version, and R. Miranda and D. Cox for providing assistance via email.

REFERENCES

- [1] Batyrev, V.V. Dual polyhedra and mirror symmetry for Calabi-Yau hypersurfaces in toric varieties. *J. Algebraic Geom.* **1994**, *3* (3), 493 - 535.
- [2] Barth, W.; Peters, C.; Van de Ven, A. *Compact Complex Surfaces*; Ergebnisse der Mathematik; Springer-Verlag: Berlin, 1984; 3. Folge, Band 4.
- [3] belcastro, s-m. *Picard Lattices of Families of K3 Surfaces*; Ph.D. dissertation; University of Michigan: Ann Arbor, 1997; Available also for download at <http://www.math.uni.edu/~smbelcas/prof.html>
- [4] Brieskorn, E. *The Milnor Lattices of the Exceptional Unimodular Singularities*; Bonner Mathematische Schriften: 1983; Vol. 150.
- [5] Cox, D.A. Picard Numbers of Surfaces in 3-Dimensional Weighted Projective Spaces. *Math. Z.* **1989**, *201*, 183 - 189.
- [6] Danilov V.I. The Geometry of Toric Varieties. *Russian Math. Surveys* **1978**, *33* (2), 97 - 154.
- [7] Dolgachev I.V. Mirror symmetry for lattice polarized K3 surfaces. *Algebraic geometry*, 4. *J. Math. Sci.* **1996**, *81* (3), 2599 - 2630.
- [8] ———. Weighted Projective Varieties. In *Group Actions and Vector Fields*; Lect. Notes in Math.; Springer-Verlag: New York, 1982; Vol. 956, 34 - 72.
- [9] Fulton, W. *Introduction to Toric Varieties*; Annals of Mathematics Studies; Princeton University Press: Princeton, 1993.
- [10] Iskovskikh, V.A.; Shafarevich, I.R. Algebraic Surfaces. In *Algebraic Geometry II*; Encyclopaedia of Math. Sci.; Springer-Verlag: New York, 1996; Vol. 35, 127 - 262.
- [11] Khovanskii, A.G. Newton Polyhedra and Toroidal Varieties. *Funct. Anal. App.* **1977**, *11*, 289 - 296.
- [12] Khovanskii, A.G. Newton Polyhedra (Resolution of Singularities). *J. Soviet Math.* **1984**, *27*, 2811 - 2830.
- [13] Kreuzer, M.; Skarke, H. Classification of Reflexive Polyhedra in Three Dimensions. *Adv. Theor. Math. Phys.* **1998**, *2* (4), 853 - 871.
- [14] Miranda, R. *The Basic Theory of Elliptic Surfaces*; ETS Editrice Pisa, ISBN 88-7741-462.
- [15] Nikulin, V. V. Integral Symmetric Bilinear Forms and Some of Their Applications. *Math. USSR-Izv.* **1980**, *14* (1), 103 - 167.
- [16] Shioda, T. On Elliptic Modular Surfaces *J. Math. Soc. Japan* **1972**, *24* (3), 20 - 59.
- [17] Yonemura, T. Hypersurface K3 Singularities. *Tôhoku Math J.* **1990**, *42*, 351 - 380.